Metaproteomic analysis of King Ghezo tomb wall (Abomey, Benin) confirms 19th century voodoo sacrifices

Philippe Charlier, Virginie Bourdin, Didier N'Dah, Mélodie Kielbasa, Olivier Pible, Jean Armengaud

Received: 4 February 2024 | Revised: 1 May 2024 | Accepted: 13 May 2024

DOI: 10.1002/pmic.202400048

Proteomics
Proteomics and Systems Biology

RESEARCH ARTICLE

Metaproteomic analysis of King Ghezo tomb wall (Abomey, Benin) confirms 19th century voodoo sacrifices

Philippe Charlier[1,2,3] | **Virginie Bourdin**[2] | **Didier N'Dah**[4] | **Mélodie Kielbasa**[5] | **Olivier Pible**[5] | **Jean Armengaud**[5]

[1]Department of research and higher education, musée du quai Branly – Jacques Chirac, Paris, France

[2]Laboratory Anthropology, Archaeology, Biology (LAAB), UFR of Health Sciences (UVSQ/Paris-Saclay University), Montigny-Le-Bretonneux, France

[3]Foundation Anthropology, Archaeology, Biology (FAAB) – Institut de France, Paris, France

[4]Département d'Histoire et d'Archéologie, Institut National des Métiers d'Art, d'Archéologie et de la Culture (INMAAC), Université d'Abomey-Calavi, Boite Postale 04 BP 431 Cotonou, République du Bénin

[5]Département Médicaments et Technologies pour la Santé (DMTS), CEA, INRAE, SPI, Université Paris-Saclay, Bagnols-sur-Cèze, France

Correspondence
Jean Armengaud, Université Paris-Saclay, CEA, INRAE, Département Médicaments et Technologies pour la Santé (DMTS), SPI, 30200, Bagnols-sur-Cèze, France.
Email: jean.armengaud@cea.fr

Funding information
French National Agency for Research (Agence Nationale de la Recherche), Grant/Award Number: ANR-20-CE34-0012; the Région Occitanie, Grant/Award Number: 21023526-DeepMicro

Abstract

The palace of King Ghezo in Abomey, capital of the ancient kingdom of Dahomey (present-day Benin), houses two sacred huts which are specific funerary structures. It is claimed that the binder in their walls is made of human blood. In the study presented here, we conceived an original strategy to analyze the proteins present on minute amounts of the cladding sampled from the inner facade of the cenotaph wall and establish their origin. The extracted proteins were proteolyzed and the resulting peptides were characterized by high-resolution tandem mass spectrometry. Over 6397 distinct molecular entities were identified using cascading searches. Starting from without a priori searches of an extended generic database, the peptide repertoire was narrowed down to the most representative organisms—identified by means of taxon-specific peptides. A wide diversity of bacteria, fungi, plants, and animals were detected through the available protein material. This inventory was used to archaeologically reconstruct the voodoo rituals of consecration and maintenance of vitality. Several indicators attested to the presence of traces of human and poultry blood in the material taken. This study shows the essential advantages of paleoproteomics and metaproteomics for the study of ancient residues from archaeological excavations or historical monuments.

KEYWORDS
archaeology, mass spectrometry, metaproteomics, paleoproteomics, proteotyping, rituals, taxonomy

1 | INTRODUCTION

The city of Abomey, capital of the Zou department in southern Benin, is located at the center of a palm- and peanut-producing area about 140 km north of Cotonou. Founded in the early 17th century [1], Abomey was the capital of the historical kingdom of Dahomey (present-day Benin), where 12 kings of the same dynasty succeeded each other between the 17th century and the beginning of the 20th century [2]. The kingdom of Dahomey was an absolute monarchy: the king governed through a centralized bureaucracy, and embodied the unchallenged pinnacle of a rigidly stratified society of royalty,

Abbreviations: LC-MS/MS, liquid chromatography-coupled to tandem mass spectrometry; TSMs, Taxon-Spectrum Matches.

commoners, and slaves [1]. Abomey—Benin's third largest city—is one of the country's greatest tourist attractions on account of the royal palace compounds and tombs. In 1944, the buildings were transformed into a historical museum [1] by the French Governor. As a consequence, the palaces of kings Glele (1814–1889) and Ghezo (date of birth unknown—1859) are open to the public [2]. The royal palaces of Abomey have been listed as UNESCO World Heritage sites since 1985.

King Ghezo, famous for his power, is traditionally presented as the ninth king of Abomey. He reigned between 1818 and 1858, and is particularly known for his numerous expeditions against the Yoruba. The main consequence of these expeditions was the end of the heavy annual tribute enslaving the kingdom of Abomey [2]. The hallmarks of King Ghezo's reign were death and warrior power. It is said that the alley leading to his hut was paved with the skulls and jawbones of defeated enemies, and that one of his thrones rested on the skulls of four defeated enemy leaders [2, 3]. Officially, Ghezo died a natural death in his palace. However, an unofficial version states that the king died during an ambush against the Yoruba. King Ghezo's palace compound includes special funerary structures, in the form of two adjoining sacred huts (*jexo*). These structures were consecrated by Ghezo to honor the memory of his father Adandozan (who reigned between 1797 and 1818). This building is unusual for its construction materials: the binder of the walls is not a standard mortar, but is claimed to be made of red oil and lustral water mixed with the blood of 41 sacrificial victims—41 being a sacred number in voodoo [2]. The victims were probably slaves or captives of enemy populations.

The kings of Abomey, like their brothers of Allada and Porto-Novo (also in present-day Benin), were God-kings, that is to say they combined temporal and spiritual power. Their culture and religion were voodoo. In this chrono-cultural context, death is only a change of state, not a total disappearance. Importantly, a barrier between the human world and the place where the body is laid (or the spirit of the deceased) can be magically delineated. This separator is part of a supernatural border, since metaphysical elements are incorporated into the physical wall. These elements include prayers, earth from a sacred place, water from a divine spring, the blood of enemies. Together, their mystical force is symbolically charged with protecting what remains of the subtle essence of the deceased king.

From 2018 to 2022 a partnership and scientific cooperation agreement between the quai Branly-Jacques Chirac museum (Paris, France), the Abomey-Calavi university (Benin), and the French Ministry of Europe and Foreign Affairs undertook archaeological excavations in the royal palaces of Abomey (AROMA mission). In the context of this mission, several evenly spaced points on the internal facade of the wall of the cenotaph were delicately scraped in to remove amount of coating. These samples could be analyzed by a number of modern high-throughput techniques to identify their constituent components.

Although genomics is the most advanced of these techniques, ancient DNA degrades easily over time depending on the storage conditions. In addition, and most importantly for this study, it cannot provide information on the source tissue. For example, DNA may simply come from the skin of people touching the wall, in the absence of any sacrificial or ritual deposit. In contrast, proteins have recently been used as biological archives in several studies.

Significance of the Study

King Ghezo's palace is located in Abomey (Benin) which was formerly the capital of the West African Kingdom of Dahomey. The special funerary structures inside this palace are unusual: the binder for the walls is not a standard mortar, but is claimed to be composed of red oil and lustral water mixed with the blood of 41 sacrificial human victims—41 being a sacred number in Voodoo. Here, we describe how we could establish the taxonomic origin of proteins from this mortar using metaproteomics. Our comprehensive inventory of protein material was used to archaeologically reconstruct voodoo consecration and vitality maintenance rituals. Several indicators attested to the presence of traces of human and poultry blood in the collected material. Thus, we confirmed that the wall binder is made of human blood, a conclusion that could not have been reached with nucleic acid sequencing approaches. We anticipate that paleoproteotyping will be further refined and used to reexamine archaeological remains more systematically.

Metaproteomics, the study of proteins from complex samples containing multiple organisms, is attracting increasing interest [4, 5]. This strategy is based on the analysis of tandem mass spectrometry data acquired on proteolyzed proteins matched against a database comprising a selection of annotated genomes to provide the best possible taxonomic coverage. The peptides identified allow taxonomic and functional characterization of the sample. The ever-expanding protein sequence databases, derived from genome sequencing, makes this approach very promising [4]. Proteotyping of organisms based on tandem mass spectrometry data has been successfully used to identify bacteria [6, 7], and more complex medical microbiota [8, 9] or environmental microbiota [10].

The capacity to identify and quantify proteins by proteomics strategies, and the advent of soft ionization techniques for high-resolution mass spectrometry have led to the emergence of paleoproteomics [11, 12]. Often compared to its sister field of paleogenomics, paleoproteomics is not yet as developed in scale or scope, but has been successfully used to retrieve biomolecular sequence data from samples [12]. Very recently, the term paleoproteotyping was proposed to refer to the application of a metaproteomics-derived approach to archaeological samples [13].

Recent advances in liquid chromatography-coupled to tandem mass spectrometry (LC-MS/MS) instrumentation in terms of sensitivity and resolution, improvements in sample preparation methods when working with minute amounts [14, 15], and the growing sophistication of data analysis strategies, mean that proteomics and metaproteomics are now in a position to play an important role in archaeology [16].

Indeed, mass spectrometry-based proteomics has already been used in a multi-omics approach to analyze artifacts [17], archaeological clay matrices [18], and ancient food [19–21]. When it comes to analyzing ancient human remains, most studies work with historic dental calculus [11, 15, 22–26], as it is a stable, long-term reservoir of proteins [27]. However, recent publications have explored proteome variations in human bones or mummified human remains [28–32]. While proteomics opens the door to the analysis of paints, coatings, binders, and patina applied to walls or objects of art in archaeology [33–35], the possibility that human elements have been incorporated into pigments or organic binders on covered surfaces has rarely been studied. A single recent publication reported the identification of human blood and bird egg proteins in a red paint covering a 1000-year-old gold mask from Peru [36].

For the study presented here, we applied an original metaproteomics strategy to test the hypothesis that human blood was present in the coating covering the wall of the sacred huts in Abomey. Our without a priori proteotyping identified the type of tissue and the origin of the biological material. From this information, and confrontations with historical and anthropological knowledge, we were able to come to a better understanding of the environment and of the magical and religious practices of the kings of Abomey.

2 | MATERIALS AND METHODS

2.1 | Sample preparation for metaproteomics

Aliquots (two 80-mg replicates) of sampled material were added to 150 µL lithium dodecyl sulfate 1X lysis buffer (Thermo) supplemented with a 1:1:1 mixture of 0.1 mm silica beads (MP Biomedical), 0.5 mm glass beads (Bertin Technologies), and 0.1 mm glass beads (Bertin Technologies), as described in the fast proteotyping of microorganisms protocol [14]. Samples were subjected to bead-beating using a Precellys Evolution instrument (Bertin Technologies). The resulting protein extracts were denatured for 5 min at 99°C. Each sample was split into six 20-µL replicates, which were submitted to electrophoresis on a NuPAGE 4%–12% Bis-Tris gel for 5 or 10 min. The proteins were treated either as a single polyacrylamide gel band (5-min migration) or four polyacrylamide gel bands resolved according to their molecular weight (10-min migration). Proteins were proteolyzed in-gel with trypsin, as recommended [37].

2.2 | NanoLC-MS/MS acquisition and interpretation

The resulting peptides were resolved by reverse phase chromatography on a Vanquish Neo UHPLC (Thermo-Fisher), and their characteristics were measured with an Exploris 480 tandem mass spectrometer operated in data-dependent acquisition mode, with parameters similar to those described elsewhere [38]. The gradient applied started with a 90-min linear 5%–25% gradient of acetonitrile in the presence of 0.1% of formic acid. This was followed by a 5-min wash with a 25%–40% linear gradient, and re-equilibration. Only ions with 2 or 3 positive charges were selected for fragmentation; a 10-s dynamic exclusion window was applied. MS/MS spectra were assigned by Mascot Daemon 2.6.1 (Matrix science) according to the previously published procedure for metaproteomics analysis of complex samples [8]. The procedure comprised three iterative searches. In the first round, the 10,000 best MS/MS spectra were selected and queried against the NCBInrS database [8]. During the second round, all MS/MS spectra were used to query a database reduced to the genera identified during the first round, and all their descendants. The third round of search was carried out against a database reduced to the species identified during the second search. The parameters were as follows: full trypsin specificity, one missed cleavage allowed, 3-ppm mass tolerance on the parent peptide ion, 0.02-Da tolerance on the secondary fragment ions, fixed modification: carboxyamidomethylation of cysteine residues, variable modifications: oxidation of methionine and proline residues. TSMs were assigned as previously defined [39], and the number of taxon-specific peptide sequences were counted at all possible taxonomical ranks, and for all taxa identified. Peptide preparation and nanoLC-MS/MS measurements were performed several times to produce a total of six representative datasets: four datasets corresponding to a single 90-min nanoLC-MS/MS run (A1, A2, B1, and B2) and two datasets corresponding to 4 × 90-min nanoLC-MS/MS runs (A3 and B3). Correspondingly, the PXD040121 comprises 12 .Raw files, 6 .mgf files, 6 .Dat files. NanoLC-MS/MS analysis of blank samples under identical conditions yielded no reliable organism identification. Adhering to best practices in proteomic analysis, each nanoLC-MS/MS run was succeeded by an analytical run devoid of peptide material injection, thereby mitigating potential carryover effects for samples of interest.

3 | RESULTS

A small quantity of dried material sampled from several points on the internal facade of the wall of the cenotaph of King Ghezo's tomb (Figure 1) was subjected to metaproteomics analysis. To check the heterogeneity of the dried material, six nanoLC-MS/MS datasets were acquired on peptides derived from proteins extracted from the very unique cultural sample, subdivided into two biological replicates, using two separate strategies that have been proven to provide extensive metaproteome coverage [40]. A total of 342,643 MS/MS spectra were acquired for the six technical and analytical replicates (Table 1). The six datasets were then independently queried against a generalist database to identify the organisms potentially present in the sample at the different taxonomical ranks. When considering all six datasets, the final query led to the assignment of 37,206 MS/MS spectra to peptide sequences. Thus, a ratio of 11% of spectra were interpreted. This proportion corresponds to the expected ratio for samples of equivalent complexity analyzed in similar experimental conditions [10].

Taxonomical information was then assigned to each of the interpreted spectra, that is, the list of taxa containing a given peptide sequence was established at all possible taxonomical ranks. The main

FIGURE 1 Illustration of the wall of King Ghezo's tomb. Panel A shows a general view of the cenotaph wall. Panel B shows specific detail of the red wall buttressed by a wood beam. Copyright: Philippe Charlier.

taxonomical features obtained are indicated in Table 1. For the sake of clarity, only the largest dataset—the B3 dataset, graphically represented in Figure 2—will be commented hereafter.

Interpretation of the 5866 peptide sequences and 10,346 Taxon-Spectrum Matches (TSMs) in this dataset indicated the presence of biological material originating from Bacteria, Eukaryota, and Archaea. A total of 4208 peptides specific to Bacteria, and 1240 peptides specific to Eukaryota were identified, compared to only 50 peptides specific to Archaea. The respective biomass ratios were obtained from the TSMs measured at the Superkingdom rank: 7006 for Bacteria, 3274 for Eukaryota, and 433 for Archaea, that is, 61%/35%/4%, respectively.

3.1 | Identification of bacterial components present in the sample

At the phylum level, Actinobacteria and Proteobacteria dominated the bacterial signal with 76% and 23% of TSMs, respectively. Twelve bacterial classes were identified: Actinobacteria, Acidimicrobiia, Thermoleophilia, Alphaproteobacteria, Deltaproteobacteria, Betaproteobacteria, Gammaproteobacteria, Thermomicrobia, Chloroflexia, Bacilli, Nitrospira, and Sphingobacteria. The proteotyping strategy was quite specific, clearly delineating a total of 40 microbial genera based on a high number of taxon-specific peptides (minimum of 8 genus-specific peptides). The most abundant of these were Nocardioides (30.7% of the bacterial biomass), Bradhyrhizobium (10.8%), Streptomyces (7.9%), Nocardia (7.9%), Pseudomonas (5.1%), Nakamurella (4.3%), and Agromyces (3.9%). In most cases, the proteotyping returned the most abundant species for each genera. Consequently, the most abundant bacterial species were *Nocardioides luteus*, *Bradyrhizobium erythrophlei*, *Nocardia thailandica*, *Streptomyces gancidicus*, and *Nakamurella multipartita*. Most of these species are environmental bacteria. Only *N. thailandica* is known to be pathogenic in humans, providing the first hint that human elements might be contained in the samples.

3.2 | Eukaryota taxa revealed by metaproteomics-based proteotyping

Five significant eukaryotic phyla were identified based on taxon-specific peptides: Chordata (64% of the eukaryotic protein biomass

TABLE 1 Main features of the six nanoLC-MS/MS datasets.

Datasets	#MS/MS	#TSMs	#Peptides	#Phyla	#Class	#Order	#Family	#Genus	#Species
A1	32647	4263	2696	8	15	25	30	31	38
A2	49439	5351	4066	18	26	43	54	58	61
A3	55755	5834	2785	16	23	39	45	49	50
B1	56781	6157	4690	16	26	48	58	68	72
B2	49573	5255	4015	14	25	46	56	61	65
B3	98448	10346	5866	19	31	46	57	65	70

#, number of entities (MS/MS spectra, TSMs, Peptides) or taxa identified.

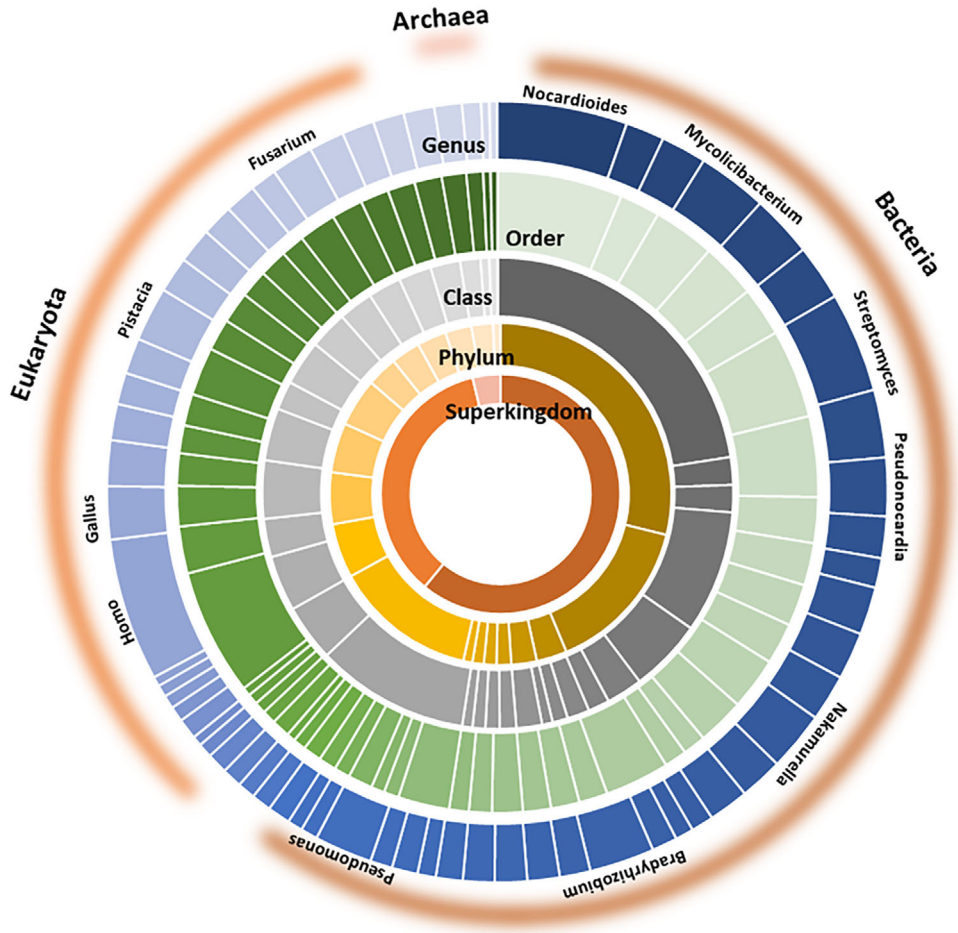

FIGURE 2 Taxonomical results obtained for dataset B3. Five taxonomical ranks (Superkingdom, Phylum, Class, Order, Genus) are represented by rings (from the inner to the outer, respectively). The number of entities identified for each of the taxonomical ranks are separated by white lines, and their width corresponds to the abundance measured (TSMs ratio). The most abundant genera are indicated.

based on TSMs), Streptophyta (13%), Ascomycota (11%), Basidiomycota (6%), and Arthropoda (6%). Trace amounts of four other phyla (Mucoromycota, Nematoda, Mollusca, and Chlorophyta) were also detected. This profile is atypical compared to a soil sample, that would contain fewer animal traces [10].

The Arthropoda signal can be explained by the presence of Diptera (Rhagoletis and Drosophila genera), Hymenoptera (Temnothorax-related ant), and arachnids (Araneus-related spider).

The plant signals were from the Anacardiaceous family, best represented by the *Pistacia vera species* (258 taxon-specific peptides).

Among the fungi detected, seven genera were distinguished, with the following representative species: *Fusarium vanettenii* (76 taxon-specific peptides, 52% of the fungus biomass), *Phlebiopsis gigantea* (15 taxon-specific peptides, 20% of the fungus biomass), *Aspergillus turcosus* (29 taxon-specific peptides, 11%), *Polyporus brumalis* (14 taxon-specific peptides, 7%), *Mycena sanguinolenta* (11 taxon-specific peptides, 2%). *Ceratobasidium* sp. AG-I (11 taxon-specific peptides, 3%), *Mortierella alpina* (10 taxon-specific peptides, 2%), and *Trichosporon asahii* (11 taxon-specific peptides, 2%).

Finally, the Chordata signal was linked to the presence of peptides originating from two types of animals: *Homo sapiens* (246 species-specific peptides, 96% of Chordata biomass), and *Gallus gallus* (23 species-specific peptides, 4% of the Chordata biomass). Thus, the presence of human elements is confirmed, we therefore examined these peptides carefully to determine their tissue origins.

3.3 | Blood is present, and its origin can be traced

The metaproteomics search of the B3 dataset revealed 5866 peptide sequences associated with 1810 possible proteins grouped into 1445 protein groups. The small number of peptides per protein group (average 2.2) is classical in metaproteomics due to the large diversity of peptides present in the sample, and the sampling effect during nanoLC-MS/MS analysis [4].

If we specifically examine the sequence coverage of the human proteins, it was higher than the average, indicating that these proteins

TABLE 2 Key proteins identified in dataset B3[a].

***Homo sapiens* proteins**				
Protein group	Protein accession	Functional description	#Peptides	Spectral count[b]
1	AFA52004.1	Keratin 1	39	456
37	**BAC85363.1**	**Immunoglobulin[c]**	**5**	**12**
38	**BAG37325.1**	**Albumin[c]**	**5**	**12**
145	**AVR43714.1**	**Hemoglobin subunit beta**	**2**	**5**
150	NP_001014364.1	Filaggrin-2	2	5
197	NP_001239546.1	Lipocalin-1 isoform 1	2	4
305	**NP_005208.1**	**Neutrophil defensin 3**	**2**	**3**
307	**QBK47576.1**	**Immunoglobulin kappa chain**	**2**	**3**
667	**BAB71634.1**	**Immunoglobulin[c]**	**1**	**1**
771	NP_057323.3	Myosin-XV	1	1
811	EAW71840.1	Myosin, heavy polypeptide 14	1	1
1282	**QEP24052.1**	**Immunoglobulin[c]**	**1**	**1**
Gallus gallus proteins				
Protein group	Protein accession	Functional description	#Peptides	Spectral count[b]
11	**NP_990820.1**	**Hemoglobin subunit beta**	**6**	**31**
47	NP_990612.1	Lysozyme C precursor	1	11
102	XP_015154748.1	Feather keratin 1-like	1	7
213	**NP_001004375.1**	**Hemoglobin subunit alpha-D**	**2**	**4**
272	XP_003643909.2	Feather keratin 3-like	1	3
368	XP_015155773.1	Citrate synthase isoform X1	3	2
472	**NP_001004376.1**	**Hemoglobin subunit alpha-A**	**2**	**1**
524	NP_001188328.1	Gallinacin-2 precursor	2	1

[a]Blood proteins are indicated in bold.
[b]Spectral count after applying peptide parsimony.
[c]Reannotation after Blast (NCBI) search.

are the most abundant contributors in the identified biomass. In total, 215 peptides were assigned to 49 human proteins (average 4.4 peptides per group). In comparison, only 21 peptides were assigned to the 12 *G. gallus* proteins detected (average 1.8 peptides per group). As shown in Table 2, the most abundant proteins from *G. gallus* were hemoglobin subunits (beta, alpha-A, and alpha-D), but feather keratins, citrate synthase, the antimicrobial gallinacin-2, and lysozyme C were also distinguished. Among the *H. sapiens* proteins, the most abundant were keratins, with 126 unambiguous peptides. Other human proteins were highlighted by this analysis, the most remarkable of which were: the hemoglobin beta subunit, four distinct immunoglobulin polypeptides, albumin, and two myosin isoforms. Peptides identifying blood proteins are highly conserved among primates. However, because no other specific peptides of simian origin were traced, the peptides identified are necessarily *H. sapiens*. Therefore, the metaproteomics-based proteotyping results undoubtedly revealed the presence of several specific blood proteins originating from *G. gallus* and *H. sapiens*. Their overall abundances—as estimated by their cumulated spectral counts—were remarkably similar (36 and 37, respectively, as indicated in Table 2).

3.4 | Complementary information from the six datasets

Although the density of information was not equivalent across the six datasets, most of the taxa identified were found to be shared, and present in similar relative biomasses. This can be seen in Figure 3, showing the highest taxonomical ranks from the heatmap of the phyla observed in the six datasets. A total of 6397 distinct molecular entities were established and 6095 peptide sequences were identified when the six datasets were merged. *H. sapiens* and *G. gallus* were systematically identified in the six datasets. Additional human blood proteins were also identified when considering the five other datasets. These included hemoglobin alpha subunit, neutrophil defensin 1, and antileukoproteinase, which is known to modulate the inflammatory and immune responses. Figure 4, Panel A shows a Venn diagram with areas proportional to the number of peptides shared between datasets. Although the mass spectrometer selects only some peptides for fragmentation among the numerous peptides available, a strong overall overlap was observed, indicating that the datasets were very similar. Figure 4, Panel B shows that blood-specific peptide-sets were found

Dataset	A1	A2	A3	B1	B2	B3
Archaea		22	36	27	26	73
Bacteria	8906	7376	3997	8813	7347	13844
Acidobacteria						13
Actinobacteria	7908	6499	3179	7123	6225	11064
Bacteroidetes						0
Chloroflexi		67	26	36	57	96
Firmicutes	21	93	121	0		24
Nitrospirae		21		33	35	65
Planctomycetes		44	28	49	28	62
Proteobacteria	977	652	643	1572	1002	2520
Eukaryota	1342	1912	2891	1939	1497	3661
Arthropoda	17	51	79	143	131	237
Ascomycota	301	209	159	296	250	371
Basidiomycota	73	83	51	130	119	207
Chlorophyta		15		13	15	30
Chordata	899	1432	2335	1280	874	2251
Bos	123					
Gallus	92	134	177	41	37	88
Homo	684	1298	2158	1239	837	2163
Cnidaria			0			
Colpodellida		17				
Mollusca		11	15	4		21
Mucoromycota		6	5	7	10	16
Nematoda		4		8	19	26
Oomycota		4	6			
Streptophyta	52	80	241	58	79	502
Total	10248	9310	6924	10779	8870	17578

FIGURE 3 Heatmap of the six datasets at the phylum rank. The number of assigned TSMs (activated parsimony) is indicated for each dataset and each taxon. Genera for the Chordata phylum are also indicated. A color is assigned depending on the number of TSMs assigned (blue to red gradient: from the lowest to the highest value).

in extractions A and B. Both samples contained *G. gallus* and *H. sapiens* peptides, with slightly more *G. gallus* in datasets A, and slightly more *H. sapiens* in datasets B (Table 3).

The 12 bacterial genera systematically identified in all six datasets were among the most abundant entities, and collectively represented 70% of the bacterial biomass. The discrepancies noted at the lowest taxonomical ranks can be explained by the combined effects of (i) lower signals, (ii) sampling effects occurring within the mass spectrometer during the analysis of highly complex mixtures of peptides, and (iii) heterogeneity of the powdered particles. The A3 dataset contained a higher diversity of plant residues: *Oryza sativa* (81 species-specific peptides), the grass *Eragrostis curvula* (6 peptides), the ornamental plant *Ipomoea nil* (7 peptides), the wild tobacco *Nicotiana attenuate* (6 peptides), the flowering plant *Rhamnella rubrinervis* (4 peptides), and the radish *Raphanus sativus* (6 species-specific peptides).

Unexpectedly, the A1 and A2 datasets indicated the presence of wheat (11 and 8 *Triticum aestivum*-specific peptides, respectively). In contrast, the B1 and B2 datasets revealed the more consensual presence of corn (19 and 20 *Zea mays*-specific peptides, respectively). *Vigna unguiculata*, cowpea, was identified only in the A1 dataset (6 species-specific peptides).

Furthermore, another fungus was also identified in dataset A1, *P. gigantea* (11 species-specific peptides). Some additional bacteria such as *Fusarium napiforme* (16 species-specific peptides) and *Fusarium euwallaceae* (39 species-specific peptides) were best identified in datasets A3 and B2, respectively. Trametes fungi were identified in the A1, B1, and B2 datasets: *Trametes cinnabarina* (11 species-specific peptides), *Trametes versicolor* (27 species-specific peptides), and *Trametes coccinea* (4 species-specific peptides), respectively. Finally, only the A1, A2, and A3 datasets contained insect-derived material, best rep-

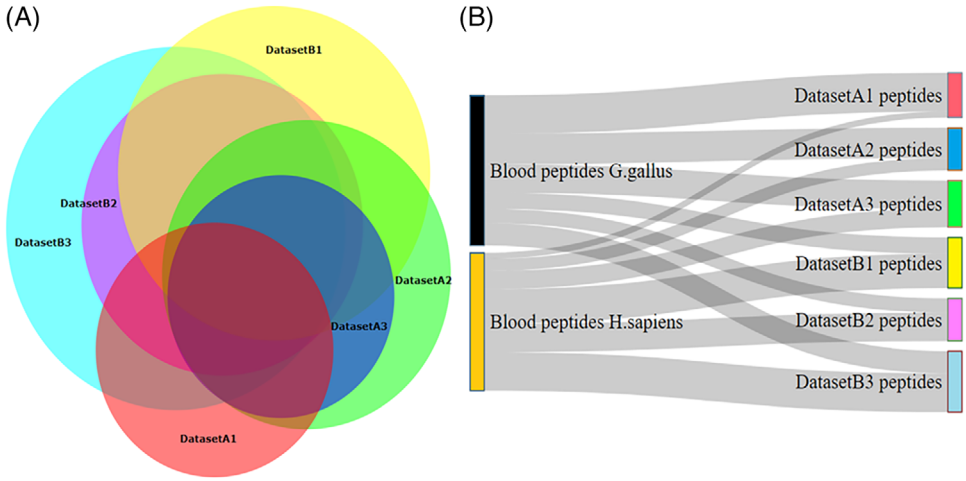

FIGURE 4 Comparison of non-redundant peptide-sets between datasets, and compared with blood subsets. Panel A: Venn diagram showing intersections between datasets. Produced with the DeepVenn tool. Panel B: Sankey diagram connecting non-redundant peptide-sets specific for *G. gallus* and *H. sapiens* blood (identified across datasets) and matching peptides in non-redundant peptide-sets for each dataset.

resented in the database as *Tribolium castaneum*, which is a worldwide stored product pest, particularly contaminating food grains. The number of species-specific peptides identified in the three datasets was 10, 11, and 8, respectively. Specifically, the A1 dataset revealed the presence of *Bos taurus* proteins (35 species-specific peptides), dominated by keratins (3 protein groups and 33 unambiguously assigned peptides) and caseins (alpha-S1-casein isoform X3, kappa casein, and beta-casein isoform X1, cumulating 10 unambiguous assigned peptides).

4 | DISCUSSION

The aim of this study was to use tandem mass spectrometry proteotyping to characterize the internal facade of the wall of King Ghezo's cenotaph in the royal palaces of Abomey to assess the presence of blood, and determining its origins. We established traces of a variety of organisms, including blood from two animals. These identifications were made possible through efforts to achieve deep coverage of the extracted peptides, leading to the identification of 6397 distinct molecular entities from the minute amounts of material available. A certain degree of heterogeneity of the sample was revealed by deploying several extractions and multiple tandem mass spectrometry measurements.

Environmental bacteria were found to constitute 68% of the samples. Among the low-abundance bacterial species, *N. thailandica*, identified by 118 taxon-specific peptides in the A3 dataset, belongs to a genus causing a variety of nocardioses in humans, with cutaneous, pulmonary, ocular, and systemic infections [41]. *Nocardia* can cause infectious disease in healthy individuals, but more than 60% of those affected have some underlying illness [42]. *N. thailandica* in particular is a rare species, linked to infections in humans in five reported cases [43]. *N. thailandica* was associated with brain disease, with abscesses detected in a 44-year-old immunocompromized American patient presenting new-onset seizures and altered mental status [42], and in a 69-year-old Japanese man who had been on long-term steroids for systemic lupus erythematosus [43]. The third case related to pulmonary nocardiosis caused by N. thailandica, and was described in a 66-year-old American patient with a history of ischemic cardiomyopathy, for

TABLE 3 Number of peptides shared between non-redundant peptide-sets.

Peptide set[a]	Blood *G. gallus*	Blood *H. sapiens*	DatasetA1	DatasetA2	DatasetA3	DatasetB1	DatasetB2	DatasetB3
Blood *G. gallus*[b]	21	0	19	15	14	8	7	11
Blood *H. sapiens*[b]		23	3	6	9	17	14	19
DatasetA1			1574	884	714	863	823	929
DatasetA2				2322	943	1338	1166	1341
DatasetA3					1433	855	830	960
DatasetB1						2716	1534	1664
DatasetB2							2208	1514
DatasetB3								3204

[a]Isomeric amino-acids I and L are undifferentiated.
[b]Peptide-sets were cumulated from results for the six datasets.

which they had received a heart transplant, and subsequent immunosuppressive therapy with tacrolimus, mycophenolate, and prednisone [44]. From these case reports, one could assume that *N. thailandica* was a purely opportunistic pathogen, affecting only patients with a compromised immune system. However, the two final case reports indicate that *N. thailandica* can also be pathogenic for immunocompetent subjects. Thus, it was isolated in the bronchoalveolar lavage of an Iranian patient admitted to hospital suffering from mild fever, weight loss, nonproductive cough, anorexia, and chronic chest pain, with no apparent evidence of immunodeficiency or HIV infection [45]. Lastly, *N. thailandica* was isolated from a Nocardia keratitis that developed consecutive to an injury incurred while working in a field in India [46]. Although *N. thailandica* has not previously been reported in Africa, it appears to be distributed worldwide, having been detected in the USA, Japan, Iran, and India. The tandem mass spectrometry proteotyping approach used here provides clear evidence that *N. thailandica* strains are present in Benin.

Fusarium spp. have been reported as a significant cause of disease in humans, especially in immunocompromized patients, who have a high risk of developing invasive life-threatening disease. A case report described disseminated fusariosis caused by *F. napiforme*, in a 60-year-old Brazilian woman with multiple myeloma after repeated cycles of chemotherapy [47]. Similarly, fungemia due to *F. napiforme* has been reported in Brazilian patients with hematologic malignancies [48]. Deep tissue infection may occur as an opportunistic hyalohyphomycosis, and wide dissemination has been reported in immunocompromized American hosts [49]. *F. napiforme* may also affect immunocompetent patients, with hypersensitivity pneumonitis diagnosed in healthy individuals in South Korea [50] and Japan [51]. Beyond its potentially pathogenic nature, *F. napiforme* was isolated from sorghum grain collected in Argentina in 1993 [52]. It is therefore not surprising to find it in a wall-coating containing traces of crops such as wheat and cowpea, all the more so as *F. napiforme* has been isolated from soil and grain samples from Australia and southern Africa [49]. In addition, the fungus *Fusarium vanettenii* is found in a broad range of environments and can cause disease on a number of crops including pea, chickpea, tomato, carrots, potato, and alfalfa. *T. asahii* (*Trichosporon beigelii*) infections, although infrequent, have been associated with a wide spectrum of clinical manifestations, ranging from mild symptoms in immunocompetent individuals, to severe systemic disease in immunocompromized patients [53]. *T. asahii* infections are the most frequently reported non-Candida fungal infections in cancer wards.

The presence of soft wheat in the sample was unexpected. Wheat was not a cereal traditionally grown in sub-Saharan Africa, unlike sorghum, millet, and cassava [54]. The consumption of bread is a relatively recent phenomenon in Black Africa. Traditionally, local cereal or tuber crops are considered adequate to compensate for the lack of wheat production [55]. The traces detected in the sample could correspond to later libations, practiced post-colonization in the 19th century, or even in the 20th century as the development of wheat crops expanded. However, it is also possible that wheat was used at the royal court of Dahomey, as King Ghezo displayed a genuine interest in his French counterpart, Napoleon III. This interest led Ghezo to enroll two of his sons in a French school in Marseille [56]. Reports also indicate that he was seduced by the beauty of the everyday objects used by the emperor [56, 57], and curious about his way of life. This interest led to the mutual exchanges of gifts: local fabrics, weapons, various utensils, and cowries from Dahomey [56]. In light of these diplomatic exchanges, flour and wheat may have circulated at the royal court of Dahomey, allowing the sovereign to taste bread and other French delicacies.

Cowpea (*V. unguiculata*) in dataset A1 is a vegetable that is widely grown and consumed in Benin, where it is the preferred grain legume, and has many uses [58, 59]. It contributes to cotton cultivation by helping to meet the food needs of a paid labor force during sowing and harvest. In addition, cowpea is used in crop rotations in association with various cereals (maize, sorghum, and millet) to allow rational fertility management. Its foliage also provides a food supplement for ruminants during the dry season [58].

The genus *Trametes* Fr. (Polyporales, Basidiomycota) consists of wood-decay fungi, and is distributed over all continents and all major climatic zones. Nine species of *Trametes* have been identified in Benin so far: *T. elegans*, *T. sanguinea*, *T. cingulata*, *T. flavida*, *T. lactinea*, *T. parvispora*, *T. polyzona*, *T. socotrana*, and *Trametes aff. Versicolor* [60]. Species of the genus *Trametes* have a long ethnomycological history as medicinal fungi in many cultures [60, 61]. An ethnomycological study of edible and medicinal mushrooms in the Mount Cameroon region showed that *Trametes* species were used as medicine [62]. Mushrooms were also used as love charms, for dispelling evil spirits, and as part of cultural festivals [62]. The maximum likelihood phylogeny of *Trametes* spp. revealed *T. cinnabarina* to share clade-likeness with *T. sanguinea*, *T. coccinea*, and *T. cingulata*. As the protein sequence database used to identify peptides cannot be comprehensive to cover all the taxonomically species, it is possible that the actual species in our sample was not one of those mentioned, but rather *T. sanguinea* or *T. cingulata*. Both these species are found in Benin, where they are used in traditional medicine or for magical protection.

The detection of Anacardiaceous plants in significant amounts is of specific interest. Such plants are known to produce a resinous or milky sap that can be nauseating or highly poisonous, as is the case for *Metopium brownei* (i.e., black poisonwood). The exact species is probably not *Pistacia vera*, as the genomes of very few related plants have been sequenced up to now.

The presence of hemoglobin and immunoglobulins from two animal species—human and chicken—raises questions about ritual practices in this chrono-cultural context: voodoo was and remains the basis of magico-religious and cultural practice in the area, and permeates the daily lives of Beninese men and women. The Abomey king was considered a God. The consecration of a fetish (wooden statue) or of a place (cave, tomb, place of memory) still obeys a very specific ritual, and organic offerings (blood, oil, or cereals in most cases) are made to the visible part of these objects or places. Offerings are food that activates the power of the consecrated object or place [2]. Blood, whether animal—in most cases—or human, is an integral part of voodoo practice. Fresh animal blood, very often chicken blood, is used to animate a fetish and breathe life into it [2]. Apart from blood, the favorite food of fetishes is *amiwo*—a mixture of palm oil and corn flour, or palm wine,

or millet beer, etc [2]. Any consecrated entity must be nourished; otherwise, its effectiveness wanes, like an animal or a human would die of hunger or thirst. Offerings of corn kernels, beans, flour, palm oil, mixtures of cereals, as well as the sacrifice of a chicken are reported during the consecration of graves and places where the memories of ancestors (*jexo*) are revered [63]. Interestingly, the modus operandi matches with all the *gallus* peptide sequences retrieved. Chicken feathers, torn from the neck, are frequently stuck into blood when it is freshly deposited on the surface of the magic object, to show the reality of the deposit of blood, which will soon turn brown and then black [2]. Small quantities of *G. gallus* blood, may correspond to sacrificial blood, as poultry are the most frequently sacrificed animal types for the consecration and/or reactivation of voodoo altars [64]. In addition to poultry proteins in dataset A1, *Bos taurus* keratins were identified in large quantities, alongside *Bos taurus* hemoglobin-related proteins, and casein—the main nitrogenous element in milk. Alpha-S1-casein isoform X3, casein kappa precursor, and beta-casein isoform X1 were linked to 47 TSMs, with 10 unambiguous peptides assigned. This significant signal could be the result of a ritualized offering of cow's milk during the construction of the wall.

From the 18th century, the long, complex and somewhat bloody voodoo ceremonies struck the imagination of Europeans, who called them "Customs" [65]. Reflecting the political and economic system of the kingdom, the Customs exalted the regime of absolute and military monarchy, where the king combined the powers of guardian of ancestor worship, principal judge, sole legislator, and supreme commander of the armies. It was probably in the 17th century that the Customs began to develop: earlier Portuguese testimonies make no mention of the existence of ritual sacrifices. Moreover, the constant wars between neighboring ethnic groups, the aim of which was to procure domestic slaves, were greatly intensified with the arrival of Europeans, who organized raids on a large scale [65]. William Snelgrave—English slave captain—reported in 1727 that it was customary in Dahomey to offer a number of captives in sacrifice; the king chose the victims himself among the prisoners.

The culmination of the Customs coincided with the pinnacle of Ghezo's reign, and the fall of Abomey in 1894 led to their almost total disappearance [65]. The "Great Customs" involved sacrifice of close to five hundred victims. They were celebrated for several weeks following the death of the reigning king, after a 2-year interregnum before the enthronement of the crown prince. During the "Custom to water the ancestors", priestesses gathered in the "House of the spirit"—a house with low, circular walls hidden by a huge palm roof—to honor the *Asê* of the ancestor, a mysterious sacred wrought iron object wrapped in ritual white cloths, onto which the blood of a few animals and sometimes one or two human victims was spilled. The small number of victims can be explained by the fact that the king felt less need to display his power among his ancestors than before his assembled people during the Great Customs [65]. The "House of Spirit" consecrated by King Ghezo for his ancestors most likely benefited from such a ritual watering ceremony.

The interior of the sacred house is laid out in the shape of an "8". It measures 4 m on the long axis, and 3 m on the short axis for each of the 2 ellipses, which are connected by a gap corresponding to 20% of their perimeter. The height of the wall is 1.60 m, with an estimated total area of 28 m^2. A limitation to the completeness of our findings is the small area of wall sampled, given that sacrificial or ritual blood was diluted with soil and other organic substances, on top of the large surface to be coated. It is likely that if new analyses were performed on other sectors of the sacred wall, they would highlight new proteins revealing other aspects of the ritual of consecration or maintenance of the vitality of this "supernatural barrier". As a consequence, it will be necessary to perform more systematic analyses of the cenotaph to obtain a comprehensive molecular profile. However, the current limitations of any methodology relying on full genome sequences available in databases will naturally improve over time, as new genome sequences are generated, especially with the inclusion of plant and fungal genomes. The high-quality MS/MS datasets recorded in the present study could be re-analyzed in the future to obtain additional insights.

In the fields of paleomicrobiology and forensics, the prevention and management of contamination are critical priorities. We implemented rigorous processes and techniques to ensure the absence of contamination of the material under examination. As a general precaution, each reagent used was new. Experiments were performed with negative controls to ensure protocol integrity and identify any potential operator-induced contamination. In our opinion, the only conceivable risk of contamination may have originated from ambient microorganisms present at the sampling site, as achieving a completely sterile environment during sampling proved unattainable. However, this level of contamination should remain minimal in comparison to the high protein content of the sample. A primary limitation of the methodology used in this study lies in the incomplete database available for interpreting the data, as numerous branches of the Tree of Life remain underrepresented in whole genome sequencing efforts. However, global genome coverage is steadily advancing, promising heightened depth and accuracy in data interpretation over time. Recent advancements in tandem mass spectrometry with high-resolution and high-speed acquisition analyzers offer expanded dimensions for proteotyping and functional metaproteomics exploration [66]. With even larger datasets, new insights will be unlock, although certain elusive details will persist. For instance, while our metaproteomic analyses identify animal species, the organisms cannot be typed by gender or stage of development. Lastly, our analysis was limited to a singular cultural sample. A comprehensive examination of the binders from different locations within the sacred huts' walls would warrant further investigation to provide a full understanding of their composition.

In conclusion, this insightful metaproteomics analysis of a wall sample from a royal tomb made it possible to confirm not only the presence of human blood, but also to reconstruct entire sections of the ritual of consecration and/or maintenance of vitality corresponding to voodoo beliefs. Notably, the detection of specific proteins such as those indicating the presence of blood is a strength of the approach, a result that cannot be obtained by metagenomics. Nevertheless, metagenomics and metaproteomics are highly complementary, as for example DNA-based identification of the victims could maybe confirm their number—symbolically 41—within the limit of contamination by the

hands of the many followers and visitors coming into contact with the wall each day. In any case, this study shows the essential advantages of proteomics (here, paleo-proteomics) for the complete study of ancient residues from archaeological excavations or historical monuments, in addition to other more traditional studies: genetics, elemental (including isotopic) and molecular analyses (oils, for example), microscopy, and other biophysical methods.

5 | ASSOCIATED MASS SPECTROMETRY DATA

The mass spectrometry and proteomics datasets are available through the ProteomeXchange Consortium via the PRIDE partner repository (https://www.ebi.ac.uk/pride/), under dataset identifiers PXD040121 anhttps://doi.org/10.6019/PXD040121.

AUTHOR CONTRIBUTIONS

Conceptualization: Philippe Charlier, Didier N'Dah, and Jean Armengaud. *Methodology*: Mélodie Kielbasa, Olivier Pible, and Jean Armengaud. *Investigation*: Philippe Charlier, Virginie Bourdin, Didier N'Dah, Mélodie Kielbasa, Olivier Pible, and Jean Armengaud. *Supervision*: Philippe Charlier and Jean Armengaud. *Writing–original draft*: Philippe Charlier, Virginie Bourdin, and Jean Armengaud. *Writing–review & editing*: Philippe Charlier, Virginie Bourdin, and Jean Armengaud.

ACKNOWLEDGMENTS

The archaeological excavations on the site of Abomey are partly financed by the musée du quai Branly—Jacques Chirac (Paris, France), the French Ministry of Europe and Foreign Affairs ("Fouilles françaises à l'étranger"), and the University of Abomey-Calavi, under the AROMA mission. The authors warmly thank Dah Constant Glélé, Franck Hounlelou, and Dr Luc Brun, for permanent local support in Abomey. J.A. is indebted to the French National Agency for Research (Agence Nationale de la Recherche, grant ANR-20-CE34-0012) and the Région Occitanie (grant 21023526-DeepMicro) for their support for the development of metaproteomics methodology within the ProGénoMix platform.

CONFLICT OF INTEREST STATEMENT

The authors declare no conflicts of interest.

DATA AVAILABILITY STATEMENT

The data that support the findings of this study will be made openly available upon publication through the ProteomeXchange Consortium via the PRIDE partner repository (https://www.ebi.ac.uk/pride/), under dataset identifiers PXD040121 anhttps://doi.org/10.6019/PXD040121.

ORCID

Jean Armengaud https://orcid.org/0000-0003-1589-445X

REFERENCES

1. Houngnikpo, M. C., & Decalo, S. (2013). *Historical dictionary of Benin (4th ed ed.)*. Lanham (Md.): Scarecrow Press, Lanham (Md.), ed. (4th ed, 2013), pp. 1 vol. (XXXVI-452 pages).
2. Charlier, P. (2020). Vaudou l'homme, la nature et les dieux Bénin. Plon, Terre humaine.
3. Sargos, C., Sargos, P., & Sargos, N. (2010). Arts et traditions d'Afrique, du profane au sacré. Agen: Hazan—Ville d'Agen.
4. Armengaud, J. (2023). Metaproteomics to understand how microbiota function: The crystal ball predicts a promising future. *Environmental Microbiology*, *25*(1), 115–125. https://doi.org/10.1111/1462-2920.16238
5. Van Den Bossche, T., Arntzen, M. O., Becher, D., Benndorf, D., Eijsink, V. G. H., Henry, C., Jagtap, P. D., Jehmlich, N., Juste, C., Kunath, B. J., Mesuere, B., Muth, T., Pope, P. B., Seifert, J., Tanca, A., Uzzau, S., Wilmes, P., Hettich, R. L., & Armengaud, J. (2021). The Metaproteomics Initiative: A coordinated approach for propelling the functional characterization of microbiomes. *Microbiome*, *9*(1), 243. https://doi.org/10.1186/s40168-021-01176-w
6. Hayoun, K., Gaillard, J. C., Pible, O., Alpha-Bazin, B., & Armengaud, J. (2020). High-throughput proteotyping of bacterial isolates by double barrel chromatography-tandem mass spectrometry based on microplate paramagnetic beads and phylopeptidomics. *Journal of Proteomics*, *226*, 103887. https://doi.org/10.1016/j.jprot.2020.103887
7. Lozano, C., Kielbasa, M., Gaillard, J. C., Miotello, G., Pible, O., & Armengaud, J. (2022). Identification and characterization of marine microorganisms by tandem mass spectrometry proteotyping. *Microorganisms*, *10*(4), 719. https://doi.org/10.3390/microorganisms10040719
8. Grenga, L., Pible, O., Miotello, G., Culotta, K., Ruat, S., Roncato, M. A., Gas, F., Bellanger, L., Claret, P. G., Dunyach-Remy, C., Laureillard, D., Sotto, A., Lavigne, J. P., & Armengaud, J. (2022). Taxonomical and functional changes in COVID-19 faecal microbiome could be related to SARS-CoV-2 faecal load. *Environmental Microbiology*, *24*(9), 4299–4316. https://doi.org/10.1111/1462-2920.160289
9. Hardouin, P., Pible, O., Marchandin, H., Culotta, K., Armengaud, J., Chiron, R., & Grenga, L. (2022). Quick and wide-range taxonomical repertoire establishment of the cystic fibrosis lung microbiota by tandem mass spectrometry on sputum samples. *Frontiers in Microbiology*, *13*, 975883. https://doi.org/10.3389/fmicb.2022.975883
10. Jouffret, V., Miotello, G., Culotta, K., Ayrault, S., Pible, O., & Armengaud, J. (2021). Increasing the power of interpretation for soil metaproteomics data. *Microbiome*, *9*(1), 195. https://doi.org/10.1186/s40168-021-01139-1
11. Hendy, J., Welker, F., Demarchi, B., Speller, C., Warinner, C., & Collins, M. J. (2018). A guide to ancient protein studies. *Nature Ecology & Evolution*, *2*(5), 791–799. https://doi.org/10.1038/s41559-018-0510-x
12. Warinner, C., Korzow Richter, K., & Collins, M. J. (2022). Paleoproteomics. *Chemical Reviews*, *122*(16), 13401–13446. https://doi.org/10.1021/acs.chemrev.1c00703
13. Bourdin, V., Charlier, P., Crevat, S., Slimani, L., Chaussain, C., Kielbasa, M., Pible, O., & Armengaud, J. (2023). Deep paleoproteotyping and microtomography revealed no heart defect nor traces of embalming in the cardiac relics of blessed Pauline Jaricot. *International Journal of Molecular Sciences*, *24*(3). https://doi.org/10.3390/ijms24033011
14. Hayoun, K., Gouveia, D., Grenga, L., Pible, O., Armengaud, J., & Alpha-Bazin, B. (2019). Evaluation of sample preparation methods for fast proteotyping of microorganisms by tandem mass spectrometry. *Frontiers in Microbiology*, *10*, 1985. https://doi.org/10.3389/fmicb.2019.01985
15. Palmer, K. S., Makarewicz, C. A., Tishkin, A. A., Tur, S. S., Chunag, A., Diimajav, E., Jamsranjav, B., & Buckley, M. (2021). Comparing the use of magnetic beads with ultrafiltration for ancient dental calculus pro-

teomics. *Journal of Proteome Research*, *20*(3), 1689–1704. https://doi.org/10.1021/acs.jproteome.0c00862
16. Merkley, E. D., Wunschel, D. S., Wahl, K. L., & Jarman, K. H. (2019). Applications and challenges of forensic proteomics. *Forensic Science International*, *297*, 350–363. https://doi.org/10.1016/j.forsciint.2019.01.022
17. Vilanova, C., & Porcar, M. (2020). Art-omics: multi-omics meet archaeology and art conservation. *Microbial Biotechnology*, *13*(2), 435–441. https://doi.org/10.1111/1751-7915.13480
18. Solazzo, C., Fitzhugh, W. W., Rolando, C., & Tokarski, C. (2008). Identification of protein remains in archaeological potsherds by proteomics. *Analytical Chemistry*, *80*(12), 4590–4597. https://doi.org/10.1021/ac800515v
19. Greco, E., El-Aguizy, O., Ali, M. F., Foti, S., Cunsolo, V., Saletti, R., & Ciliberto, E. (2018). Proteomic analyses on an Ancient Egyptian Cheese and biomolecular evidence of brucellosis. *Analytical Chemistry*, *90*(16), 9673–9676. https://doi.org/10.1021/acs.analchem.8b02535
20. Hong, C., Jiang, H., Lu, E., Wu, Y., Guo, L., Xie, Y., Wang, C., & Yang, Y. (2012). Identification of milk component in ancient food residue by proteomics. *PLoS ONE*, *7*(5), e37053. https://doi.org/10.1371/journal.pone.0037053
21. Maixner, F., Turaev, D., Cazenave-Gassiot, A., Janko, M., Krause-Kyora, B., Hoopmann, M. R., Kusebauch, U., Sartain, M., Guerriero, G., O'Sullivan, N., Teasdale, M., Cipollini, G., Paladin, A., Mattiangeli, V., Samadelli, M., Tecchiati, U., Putzer, A., Palazoglu, M., Meissen, J., & Zink, A. (2018). The iceman's last meal consisted of fat, wild meat, and cereals. *Current Biology*, *28*(14), 2348-2355 e2349. https://doi.org/10.1016/j.cub.2018.05.067
22. Bleasdale, M., Richter, K. K., Janzen, A., Brown, S., Scott, A., Zech, J., Wilkin, S., Wang, K., Schiffels, S., Desideri, J., Besse, M., Reinold, J., Saad, M., Babiker, H., Power, R. C., Ndiema, E., Ogola, C., Manthi, F. K., Zahir, M., & Boivin, N. (2021). Ancient proteins provide evidence of dairy consumption in eastern Africa. *Nature Communications*, *12*(1), 632. https://doi.org/10.1038/s41467-020-20682-3
23. Fotakis, A. K., Denham, S. D., Mackie, M., Orbegozo, M. I., Mylopotamitaki, D., Gopalakrishnan, S., Sicheritz-Pontén, T., Olsen, J. V., Cappellini, E., Zhang, G., Christophersen, A., Gilbert, M. T. P., & Vagene, A. J. (2020). Multi-omic detection of Mycobacterium leprae in archaeological human dental calculus. *Philosophical Transactions of the Royal Society of London. Series B: Biological Sciences*, *375*(1812), 20190584. https://doi.org/10.1098/rstb.2019.0584
24. Geber, J., Tromp, M., Scott, A., Bouwman, A., Nanni, P., Grossmann, J., Hendy, J., & Warinner, C. (2019). Relief food subsistence revealed by microparticle and proteomic analyses of dental calculus from victims of the Great Irish Famine. *Proceedings of the National Academy of Sciences of the United States of America*, *116*(39), 19380–19385. https://doi.org/10.1073/pnas.1908839116
25. Jersie-Christensen, R. R., Lanigan, L. T., Lyon, D., Mackie, M., Belstrom, D., Kelstrup, C. D., Fotakis, A. K., Willerslev, E., Lynnerup, N., Jensen, L. J., Cappellini, E., & Olsen, J. V. (2018). Quantitative metaproteomics of medieval dental calculus reveals individual oral health status. *Nature Communications*, *9*(1), 4744. https://doi.org/10.1038/s41467-018-07148-3
26. Velsko, I. M., Fellows Yates, J. A., Aron, F., Hagan, R. W., Frantz, L. A. F., Loe, L., Martinez, J. B. R., Chaves, E., Gosden, C., Larson, G., & Warinner, C. (2019). Microbial differences between dental plaque and historic dental calculus are related to oral biofilm maturation stage. *Microbiome*, *7*(1), 102. https://doi.org/10.1186/s40168-019-0717-3
27. Mackie, M., Hendy, J., Lowe, A. D., Sperduti, A., Holst, M., Collins, M. J., & Speller, C. F. (2017). Preservation of the metaproteome: variability of protein preservation in ancient dental calculus. *Science & Technology of Archaeological Research*, *3*(1), 74–86. https://doi.org/10.1080/20548923.2017.1361629
28. Multari, D. H., Ravishankar, P., Sullivan, G. J., Power, R. K., Lord, C., Fraser, J. A., & Haynes, P. A. (2022). Proteomics dataset from 26th Dynasty Egyptian mummified remains sampled using minimally invasive skin sampling tape strips. *Data Brief*, *45*, 108562. https://doi.org/10.1016/j.dib.2022.108562
29. Procopio, N., Chamberlain, A. T., & Buckley, M. (2017). Intra- and inter-skeletal proteome variations in fresh and buried bones. *Journal of Proteome Research*, *16*(5), 2016–2029. https://doi.org/10.1021/acs.jproteome.6b01070
30. Procopio, N., Hopkins, R. J. A., Harvey, V. L., & Buckley, M. (2021). Proteome variation with collagen yield in ancient bone. *Journal of Proteome Research*, *20*(3), 1754–1769. https://doi.org/10.1021/acs.jproteome.0c01014
31. Shaw, B., Burrell, C. L., Green, D., Navarro-Martinez, A., Scott, D., Daroszewska, A., van 't Hof, R., Smith, L., Hargrave, F., Mistry, S., Bottrill, A., Kessler, B. M., Fischer, R., Singh, A., Dalmay, T., Fraser, W. D., Henneberger, K., King, T., Gonzalez, S., & Layfield, R. (2019). Molecular insights into an ancient form of Paget's disease of bone. *Proceedings of the National Academy of Sciences of the United States of America*, *116*(21), 10463–10472. https://doi.org/10.1073/pnas.1820556116
32. Welker, F., Hajdinjak, M., Talamo, S., Jaouen, K., Dannemann, M., David, F., Julien, M., Meyer, M., Kelso, J., Barnes, I., Brace, S., Kamminga, P., Fischer, R., Kessler, B. M., , Pääbo, S., Collins, M. J., & Hublin, J. J. (2016). Palaeoproteomic evidence identifies archaic hominins associated with the Chatelperronian at the Grotte du Renne. *Proceedings of the National Academy of Sciences*, *113*(40), 11162–11167. https://doi.org/10.1073/pnas.1605834113
33. Mukhopadhyay, R. (2006). Proteomics reveals proteins in paint. *Analytical Chemistry*, *78*(5), 1379. https://doi.org/10.1021/ac069378r
34. Roldan, C., Murcia-Mascaros, S., Lopez-Montalvo, E., Vilanova, C., & Porcar, M. (2018). Proteomic and metagenomic insights into prehistoric Spanish Levantine Rock Art. *Scientific Reports*, *8*(1), 10011. https://doi.org/10.1038/s41598-018-28121-6
35. Villa, P., Pollarolo, L., Degano, I., Birolo, L., Pasero, M., Biagioni, C., Douka, K., Vinciguerra, R., Lucejko, J. J., & Wadley, L. (2015). A milk and ochre paint mixture used 49,000 years ago at Sibudu, South Africa. *PLoS ONE*, *10*(6), e0131273. https://doi.org/10.1371/journal.pone.0131273
36. Pires, E., Carvalho, L. D. C., Shimada, I., & McCullagh, J. (2021). Human blood and bird egg proteins identified in red paint covering a 1000-year-old gold mask from Peru. *Journal of Proteome Research*, *20*(11), 5212–5217. https://doi.org/10.1021/acs.jproteome.1c00472
37. Rubiano-Labrador, C., Bland, C., Miotello, G., Guerin, P., Pible, O., Baena, S., & Armengaud, J. (2014). Proteogenomic insights into salt tolerance by a halotolerant alpha-proteobacterium isolated from an Andean saline spring. *Journal of Proteomics*, *97*, 36–47. https://doi.org/10.1016/j.jprot.2013.05.020
38. Lozano, C., Grenga, L., Gallais, F., Miotello, G., Bellanger, L., & Armengaud, J. (2023). Mass spectrometry detection of monkeypox virus: Comprehensive coverage for ranking the most responsive peptide markers. *Proteomics*, *23*(2), e2200253. https://doi.org/10.1002/pmic.202200253
39. Pible, O., Allain, F., Jouffret, V., Culotta, K., Miotello, G., & Armengaud, J. (2020). Estimating relative biomasses of organisms in microbiota using "phylopeptidomics". *Microbiome*, *8*(1), 30. https://doi.org/10.1186/s40168-020-00797-x
40. Van Den Bossche, T., Kunath, B. J., Schallert, K., Schape, S. S., Abraham, P. E., Armengaud, J., Arntzen, M. Ø., Bassignani, A., Benndorf, D., Fuchs, S., Giannone, R. J., Griffin, T. J., Hagen, L. H., Halder, R., Henry, C., Hettich, R. L., Heyer, R., Jagtap, P., Jehmlich, N., & Muth, T. (2021). Critical Assessment of MetaProteome Investigation (CAMPI): a multi-laboratory comparison of established workflows. *Nature Communications*, *12*(1), 7305. https://doi.org/10.1038/s41467-021-27542-8
41. Reddy, A. K., Garg, P., & Kaur, I. (2010a). Speciation and susceptibility of Nocardia isolated from ocular infections. *Clinical Microbiology and Infection*, *16*(8), 1168–1171. https://doi.org/10.1111/j.1469-0691.2009.03079.x

42. Yagi, R., Ooi, Y., Nonoguchi, N., & Wanibuchi, M. (2022). Brain abscess caused by *Nocardia thailandica* infection in systemic lupus erythematosus patient with steroid therapy. *Surgical Neurology International*, *13*, 126. https://doi.org/10.25259/SNI_78_2022
43. Effendi, M., Tirmizi, S., McManus, D., Huttner, A. J., Peaper, D. R., & Topal, J. E. (2021). *Nocardia thailandica* brain abscess in an immunocompromised patient. *Case Reports in Infectious Diseases*, *2021*, 6620049. https://doi.org/10.1155/2021/6620049
44. Canterino, J., Paniz-Mondolfi, A., Brown-Elliott, B. A., Vientos, W., Vasireddy, R., Wallace, R. J., Jr., & Campbell, S. (2015). *Nocardia thailandica* pulmonary nocardiosis in a post-solid organ transplant patient. *Journal of Clinical Microbiology*, *53*(11), 3686–3690. https://doi.org/10.1128/JCM.00959-15
45. Bourbour, S. P., Keikha, M. M., & Faghri, J. P. (2018). First report of the isolation of *Nocardia thailandica* from the bronchoalveolar lavage of a patient in Iran. *The Iranian Journal of Medical Sciences*, *43*(5), 560–563. https://www.ncbi.nlm.nih.gov/pubmed/30214111
46. Reddy, A. K., Garg, P., & Kaur, I. (2010b). Spectrum and clinicomicrobiological profile of Nocardia keratitis caused by rare species of Nocardia identified by 16S rRNA gene sequencing. *Eye (Lond)*, *24*(7), 1259–1262. https://doi.org/10.1038/eye.2009.299
47. de Souza, M., Matsuzawa, T., Lyra, L., Busso-Lopes, A. F., Gonoi, T., Schreiber, A. Z., Kamei, K., Moretti, M. L., & Trabasso, P. (2014). *Fusarium napiforme* systemic infection: case report with molecular characterization and antifungal susceptibility tests. *Springerplus*, *3*, 492. https://doi.org/10.1186/2193-1801-3-492
48. Moretti, M. L., Busso-Lopes, A. F., Tararam, C. A., Moraes, R., Muraosa, Y., Mikami, Y., Gonoi, T., Taguchi, H., Lyra, L., Reichert-Lima, F., Trabasso, P., de Hoog, G. S., Al-Hatmi, A. M. S., Schreiber, A. Z., & Kamei, K. (2018). Airborne transmission of invasive fusariosis in patients with hematologic malignancies. *PLoS ONE*, *13*(4), e0196426. https://doi.org/10.1371/journal.pone.0196426
49. Melcher, G. P., McGough, D. A., Fothergill, A. W., Norris, C., & Rinaldi, M. G. (1993). Disseminated hyalohyphomycosis caused by a novel human pathogen, *Fusarium napiforme*. *Journal of Clinical Microbiology*, *31*(6), 1461–1467. https://doi.org/10.1128/jcm.31.6.1461-1467.1993
50. Lee, S. K., Kim, S. S., Nahm, D. H., Park, H. S., Oh, Y. J., Park, K. J., Kim, S. O., & Kim, S. J. (2000). Hypersensitivity pneumonitis caused by *Fusarium napiforme* in a home environment. *Allergy*, *55*(12), 1190–1193. https://doi.org/10.1034/j.1398-9995.2000.00650.x
51. Unoura, K., Miyazaki, Y., Sumi, Y., Tamaoka, M., Sugita, T., & Inase, N. (2011). Identification of fungal DNA in BALF from patients with home-related hypersensitivity pneumonitis. *Respiratory Medicine*, *105*(11), 1696–1703. https://doi.org/10.1016/j.rmed.2011.07.009
52. Gonzalez, H. H., Martinez, E. J., & Resnik, S. L. (1997). Fungi associated with sorghum grain from Argentina. *Mycopathologia*, *139*(1), 35–41. https://doi.org/10.1023/a:1006803901969
53. Wolf, D. G., Falk, R., Hacham, M., Theelen, B., Boekhout, T., Scorzetti, G., Shapiro, M., Block, C., Salkin, I. F., & Polacheck, I. (2001). Multidrug-resistant *Trichosporon asahii* infection of nongranulocytopenic patients in three intensive care units. *Journal of Clinical Microbiology*, *39*(12), 4420–4425. https://doi.org/10.1128/JCM.39.12.4420-4425.2001
54. Portères, R. (1955). L'Introduction du Maïs en Afrique. *Journal d'agriculture tropicale et de botanique appliquée*, *2*(5-6), 221–231.
55. Boutrais, J. (1982). Une agriculture sans paysans : la grande culture du blé au Cameroun. *ecoru*, *147*(1), 51–54. https://doi.org/10.3406/ecoru.1982.2835
56. Beaujean, G. (2022). Le cadeau dans les relations diplomatiques du royaume du Danhomè au XIXe siècle. *Politique africaine*, *165*(1). https://doi.org/10.3917/polaf.165.0073
57. Répin, P.-C. (1971). Voyage au Dahomey… 1860 [i.e. 1856] ([Reprod.] ed.). Paris: Hachette.
58. Baco, M. N., Ahanchedé, A., Bello, S., Dansi, A., Vodouhè, R., Biaou, G., & Lescure, J.-P. (2008). Évaluation des pratiques de gestion de la diversité du niébé (*Vigna unguiculata*) : une tentative méthodologique expérimentée au Bénin. *Cahiers Agricultures*, *17*(2), 2. https://doi.org/10.1684/agr.2008.0169
59. Gbaguidi, A. A., Assogba, P., Dansi, M., Yedomonhan, H., & Dansi, A. (2015). Caractérisation agromorphologique des variétés de niébé cultivées au Bénin. *International Journal of Biological and Chemical Sciences*, *9*(2), 1050–1066. https://doi.org/10.4314/ijbcs.v9i2
60. Olou, B. A., Krah, F. S., Piepenbring, M., Yorou, N. S., & Langer, E. (2020). Diversity of Trametes (Polyporales, Basidiomycota) in tropical Benin and description of new species Trametes parvispora. *MycoKeys*, *65*, 25–47. https://doi.org/10.3897/mycokeys.65.47574
61. Cui, D. Z., Zhao, M., Yang, H. Y., Wang, C. I., & Dai, H. B. (2011). Molecular phylogeny of Trametes and related genera based on internal transcribed spacer (ITS) and nearly complete mitochondrial small subunit ribosomal DNA (mt SSU rDNA) sequences. *African Journal of Biotechnology*, *10*(79), 18111–18121. https://doi.org/10.4314/ajb.v10i79
62. Kinge, T. R., Tabi, E. M., Mih, A. M., Enow, E. A., Njouonkou, L., & Nji, T. M. (2011). Ethnomycological studies of edible and medicinal mushrooms in the Mount Cameroon region (Cameroon, Africa). *International Journal of Medicinal Mushrooms*, *13*(3), 299–305. https://doi.org/10.1615/intjmedmushr.v13.i3.100
63. Diallo, J. (1988). Les rites funéraires. In Loge de perfection "Le parvis de France"—Sous les auspices du Suprême conseil de France (Ed.), *Les travaux du Parvis de France: 5985-5988* (pp. 326). Etrechy: Ed. du soleil natal.
64. Beaujean-Baltzeer, G. (2007). Du trophée à l'œuvre : parcours de cinq artefacts du royaume d'Abomey. Gradhiva. Revue d'anthropologie et d'histoire des arts., *6*(6), 70–85. https://doi.org/10.4000/gradhiva.987
65. Coquery-Vidrovitch, C. (1964). La fête des coutumes au Dahomey : historique et essai d'interprétation. *Annales—Economies, Sociétés, Civilisations*, *19*(4), 696–716. https://doi.org/10.3406/ahess.1964.421199
66. Dumas, T., Martinez Pinna, R., Lozano, C., Radau, S., Pible, O., Grenga, L., & Armengaud, J. (2024). The astounding exhaustiveness and speed of the Astral mass analyzer for highly complex samples is a quantum leap in the functional analysis of microbiomes. *Microbiome*, *12*(1), 46. https://doi.org/10.1186/s40168-024-01766-4

How to cite this article: Charlier, P., Bourdin, V., N'Dah, D., Kielbasa, M., Pible, O., & Armengaud, J. (2024). Metaproteomic analysis of King Ghezo tomb wall (Abomey, Benin) confirms 19th century voodoo sacrifices. *Proteomics*, e2400048. https://doi.org/10.1002/pmic.202400048